

Lattice-Boltzmann Simulation of Red Blood Cell and Drug Delivery Inside the Carotid Artery

Javad Alinejad and Keivan Fallah

Department of Mechanical Engineering, Sari Branch, Islamic Azad University, Sari, Iran

*Corresponding Author's E-mail: alinejad_javad@iausari.ac.ir

Abstract

The propose of this paper is to combine the lattice Boltzmann (LB) equation and immersed boundary (IB) method to simulate the red blood cell (RBC) behavior and the blood flow inside the carotid artery. The behavior and deformation of a RBC and the streamlines are obtained. The effects of emboly on the fluid flow have been investigated. The results show that the drug delivery is effectively changed with the quality of injection. The numerical results are compared with previous study indicate that LB method can evaluate the RBC membrane behavior and velocity field in an artery with a good accuracy.

Keywords: Blood flow, Lattice Boltzmann, red blood cell, emboly, drug delivery.

1. Introduction

The simulation of complex flows in vascular passages such as carotid artery has been a major topic of research. The lattice Boltzmann method (LBM) is a powerful numerical technique based on kinetic theory for simulating fluid flows and modeling the physics in fluids [2, 8, 11 and 12]. In comparison with the conventional CFD methods, the advantages of LBM include simple calculation procedure, simple and efficient implementation for parallel computation, easy and robust handling of complex geometries. Boltzmann kinetic equation, and the result is a very elegant and simple evolution equation for a discrete distribution function, or discrete population $f_i(x, t) = f(x, c, t)$, which describes the probability to find a particle at lattice position x at time t , moving with speed c_i . With respect to the more conventional numerical methods commonly used for the study of fluid flow situations, the kinetic nature of LBM introduces several advantages, including easy implementation of boundary conditions and fully parallel algorithms. In addition, in macroscopic CFD methods, the pressure field is typically obtained by solving the Poisson or Poisson-like equations derived from incompressible N-S equations; this is normally of time consuming; whereas the pressure distributions can be obtained conveniently in the LBM by solving an extremely simple equation of state. Moreover, the convection operator is linear, and the translation of the microscopic distribution function in to the macroscopic quantities consists of simple arithmetic calculations. Blood flow simulation has been studied in previous literatures. Urquiza et al. [18] implement a multidimensional 3D–1D FEM model of the whole arterial. Specially to model large extended zones whereas localized three-dimensional models have been often implemented to study arterial flow in more detailed aspects [15]. Deschamps et al. [19] simulate directly the blood flow inside the extracted surface without losing any complicated details and without building additional grids. In the present study, an extrapolation Method based on Gou et al. [21] is used to simulate blood flow inside carotid artery. The method combined with the velocity boundary presented in Mei et al. [16] can indeed achieve

second order accuracy for velocity on the curved wall. Also, the immersed boundary method is employed to incorporate the fluid membrane interaction between the fluid field and deformable cells. Deformability of the RBC plays a major role in its behavior in the flow. This method enables one to simulate problems with particle deformation and fluid-structure deformation. The cell membrane is treated as a neo-Hookeanvisco-elastic material. The simulation results are also compared with previous research.

2. Lattice Boltzmann method

The lattice kinetic theory and especially the lattice Boltzmann method have been developed as significantly successful alternative numerical approaches for the solution of a wide class of problems [5, 10, and 17]. The LBM is derived from lattice gas methods and can be regarded as a first order explicit discretization of the Boltzmann equation in phase space. This method (LBM) is a powerful numerical technique, based on kinetic theory, for simulating fluid flow [1, 5, and 9] and heat transfer [4 and 20], and has many advantages in comparison with conventional CFD methods mentioned previously. In contrast with the classical macroscopic Navier–Stokes (NS) approach, the lattice Boltzmann method uses a mesoscopic simulation model to simulate fluid flow [4]. It uses modeling of the movement of fluid particles to capture macroscopic fluid quantities, such as velocity and pressure. In this approach, the fluid domain is made discrete in uniform Cartesian cells, each one of which holds a fixed number of Distribution Functions (DF) that represent the number of fluid particles moving in these discrete directions. Hence depending on the dimension and number of velocity directions, there are different models that can be used. The present study examined two-dimensional (2-D) flow and a 2-D square lattice with nine velocities (D2Q9 model). The velocity vectors, $c_0 \dots c_8$ of the D2Q9 model are shown in figure 1. For each velocity vector, a particle DF is stored. The velocities of the D2Q9 model are:

$$c_k = \begin{cases} (0,0) & k = 0 \\ (\pm 1, 0) & k = 1, 2, 3, 4 \\ (\pm 1, \pm 1) & k = 5, 6, 7, 8 \end{cases}$$

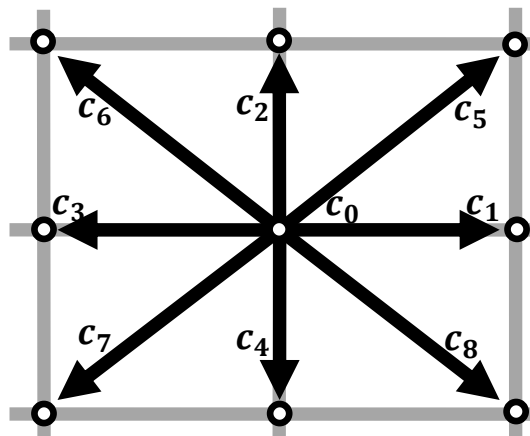


Figure 1: 2-D 9-velocity lattice (D2Q9) model.

Where $c = \Delta x / \Delta t$ and k is the Lattice velocity direction. The LB model used in the present work is the same as that employed in [4]. The DFs are calculated by solving the Lattice Boltzmann Equation (LBE), which is a special discretization of the kinetic Boltzmann equation. After introducing Bhatnagar–Gross–Krook (BGK) approximation, the Boltzmann equation can be formulated as below [13]:

$$f_k(\mathbf{x} + \mathbf{c}_k \Delta t, t + \Delta t) = f_k(\mathbf{x}, t) + \frac{\Delta t}{\tau} [f_k^{eq}(\mathbf{x}, t) - f_k(\mathbf{x}, t)] + \Delta t \mathbf{c}_k F_k \tag{1}$$

Where Δt denotes lattice time step, c_k is the discrete lattice velocity in direction k , τ denotes the lattice relaxation time, f_k^{eq} is the equilibrium DF, and F_k is the external force in the direction of the lattice velocity. Equilibrium DFs are calculated as:

$$f_k^{eq} = \omega_k \rho \left[1 + \frac{c_k \cdot \mathbf{u}}{c_s^2} + \frac{1}{2} \frac{(c_k \cdot \mathbf{u})^2}{c_s^4} - \frac{1}{2} \frac{u^2}{c_s^2} \right] \tag{2}$$

Where the weights ω_k are $\omega_k = 4/9$ for $k = 0$, $\omega_k = 1/9$ for $k = 1, 2, 3, 4$ and $\omega_k = 1/36$ for $k = 5, 6, 7, 8$; and $c_s = c_k/\sqrt{3}$ is the lattice speed of sound. The macroscopic fluid variable densities and velocities are computed as the first two moments of the distribution functions for each cell:

$$\rho = \sum_{k=0}^8 f_k, \quad \mathbf{u} = \frac{1}{\rho} \sum_{k=0}^8 f_k \mathbf{c}_k \tag{3}$$

This model is explained in more detail in [13].

3. Curved boundary treatment

Consider Figure 2 is a part of arbitrary curved wall geometry, where the black small circles on the boundary x_w , the open circles represent the boundary nodes in the fluid region x_f and the grey circles indicate those in the solid region x_b . In the boundary condition $\tilde{f}(x_b, t)$ is needed to perform the streaming steps on fluid nodes x_f . The fraction of an intersected link in the fluid region Δ is defined by:

$$\Delta = \frac{\|\mathbf{x}_f - \mathbf{x}_w\|}{\|\mathbf{x}_f - \mathbf{x}_b\|} \tag{4}$$

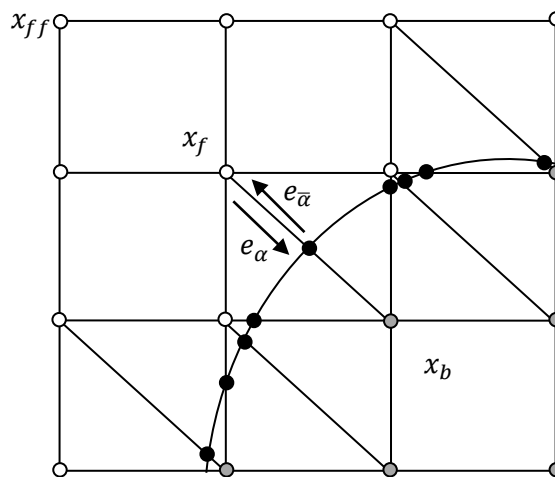


Figure 2: Layout of the regularly spaced lattices and curved wall boundary

The standard (half-way) bounce back no-slip boundary conditional ways assumes a delta value of 0.5 to the boundary wall (Figure3a). Due to the curved boundaries, delta values in the interval of (0,1) are now possible. Figure 3b shows the bounce back behavior of a surface with a delta value smaller than 0.5 and Figure 3c shows the bounce back behavior of a wall with delta bigger than 0.5. In all three cases, there flected distribution function $\tilde{f}_{\alpha}(x, t + \Delta t)$ at x_f is unknown. Since the fluid particles in the LBM a real ways considered to move on a cell length per time step, the fluid particles would come to rest at an intermediate node x_i . In order to calculate the reflected distribution function in node x_f , an inter pollution scheme has to be applied. For treating velocity field in curved boundaries, the method is based on the method reported in [21].

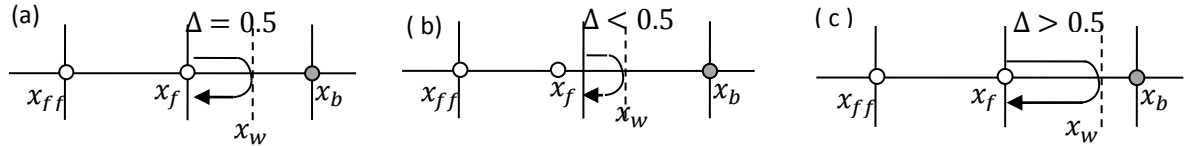


Figure 3: Illustration of the bounce-back boundary conditions. (a) $\Delta = 1/2$, (b) $\Delta < 1/2$, (c) $\Delta > 1/2$

To calculate the distribution function in the solid region $\tilde{f}_\alpha(x_b, t)$ based upon the boundary nodes in the fluid region, the bounce-back boundary conditions combined with interpolations including a one-half grid spacing correction at the boundaries [22]. Then the Chapman-Enskog expansion for the post-collision distribution function is conducted as

$$\tilde{f}_\alpha(x_b, t + \Delta t) = (1 - \lambda)\tilde{f}_\alpha(x_f, t + \Delta t) + \lambda f_\alpha^0(x_b, t + \Delta t) - 2 \frac{3}{c^2} \omega_\alpha \rho(x_f, t + \Delta t) \mathbf{e}_\alpha \cdot \mathbf{u}_w \quad (5)$$

Where

$$f_\alpha^0(x_b, t + \Delta t) = f_\alpha^{eq}(x_f, t + \Delta t) + \frac{3}{c^2} \omega_\alpha \rho(x_f, t + \Delta t) \mathbf{e}_\alpha (\mathbf{u}_{bf} - \mathbf{u}_f) \quad (6)$$

$$\mathbf{u}_{bf} = \mathbf{u}_{ff}, \lambda = \frac{2\Delta - 1}{\tau_m - 2} \quad \text{if } 0 < \Delta \leq \frac{1}{2} \quad (7a)$$

$$\mathbf{u}_{bf} = \left(1 - \frac{3}{2\Delta}\right) \mathbf{u}_f + \frac{3}{2\Delta} \mathbf{u}_w, \lambda = \frac{2\Delta - 1}{\tau_m + \frac{1}{2}} \quad \text{if } \frac{1}{2} < \Delta \leq 1 \quad (7b)$$

4. Immersed boundary

Immersed boundary method is extracted from this principle that deformation and motion of the boundary create a force that tend to return the boundary to its primary shape or position. Relationship between the membrane and the fluid are expressed by the local distribution membrane forces. For satisfaction non-slip boundary condition, the membrane and fluid velocity must be the same, thus the local fluid force term is calculated as following:

$$F_k = \left(\frac{1}{1 - 2\tau}\right) \omega_k \left[\frac{(\mathbf{c}_k - \mathbf{u})}{c_s^2} + \frac{(\mathbf{c}_k \cdot \mathbf{u})}{c_s^4} \mathbf{c}_k \right] f \quad (8)$$

Relationship between fluid flow and immersed boundary is expressed by membrane force as the following form [22],

$$f(x, t) = \int_\Gamma F(s, t) \delta(x - X(s, t)) ds \quad (9)$$

Where f is the density of force, F is the membrane force and s follows the immersed boundary nodes path. Neo-Hookean equation has been used as a structural model for the membrane cell in this article. The strain energy function is explained as:

$$W^{NH} = E(\varepsilon_1^2 + \varepsilon_2^2 + \varepsilon_1^{-2} \varepsilon_2^{-2}) \quad (10)$$

For the red blood cell tension along calculated as below:

$$T = \frac{E}{\varepsilon^{3/2}}(\varepsilon^3 - 1); \quad \varepsilon_1 = \varepsilon_2 \tag{11}$$

And finally the membrane force which is the stress resultant of adjacent nodes of (i, j), can be calculated as follows:

$$F = T_i e_i - T_j e_j \tag{12}$$

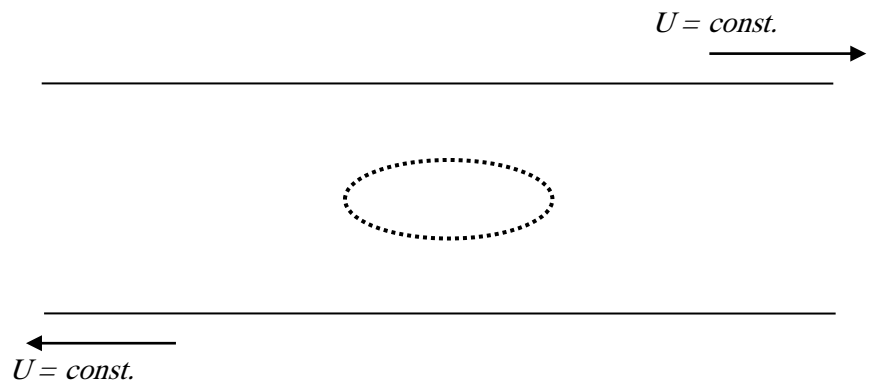
5. Code validation

For the simulation of red blood cells in shear flow different parameters values have been determined in accordance with table 1.

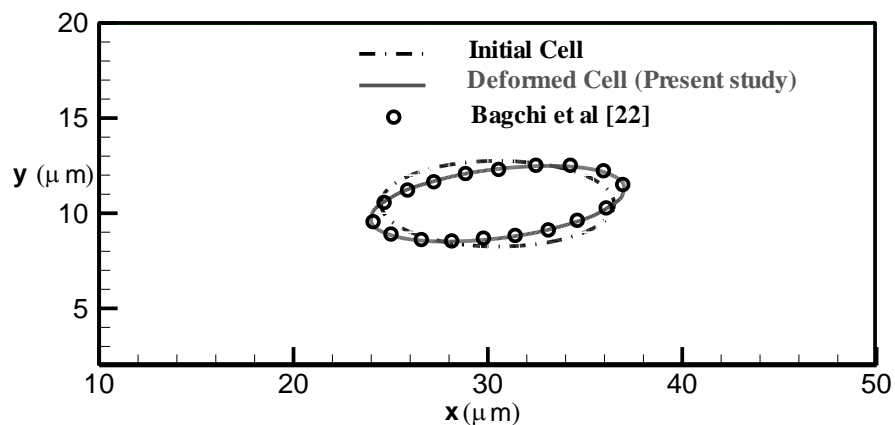
Table 1: Physical and dimensional parameters used in the simulations

Cell radius	Vessel diameter	E_s	$\dot{\gamma}$	Re	$\mu_p = 1.2 \text{ cp}$	$\lambda = \mu_c / \mu_p$
$6 \mu m$	$20 \mu m$	$1.2 \times 10^{-3} \text{ dyn/cm}$	4.2 s^{-1}	1.26×10^{-4}	$\mu_c = 6 \text{ cp}$	5

As can be seen in Figure 4, the red blood cell is placed in the Centre of the channel and the upper and lower walls move with fixed speed in opposite direction. To validate the results the deformation of elliptical red blood cell was compared by Bagchiet al[14] simulation. Comparison shows good agreement between the present results and previous work.



(a)



(b)

Figure 4: (a) The physical model, (b) the deformation of elliptical blood cell

6. Results and discussion

Various articles have presented the different geometry for red blood cells. In Figure 5, we have displayed deformation of different geometry in shear flow to show the ability of our mentioned method. Also deformation of red blood cells during the motion in a channel was shown in figure 6.

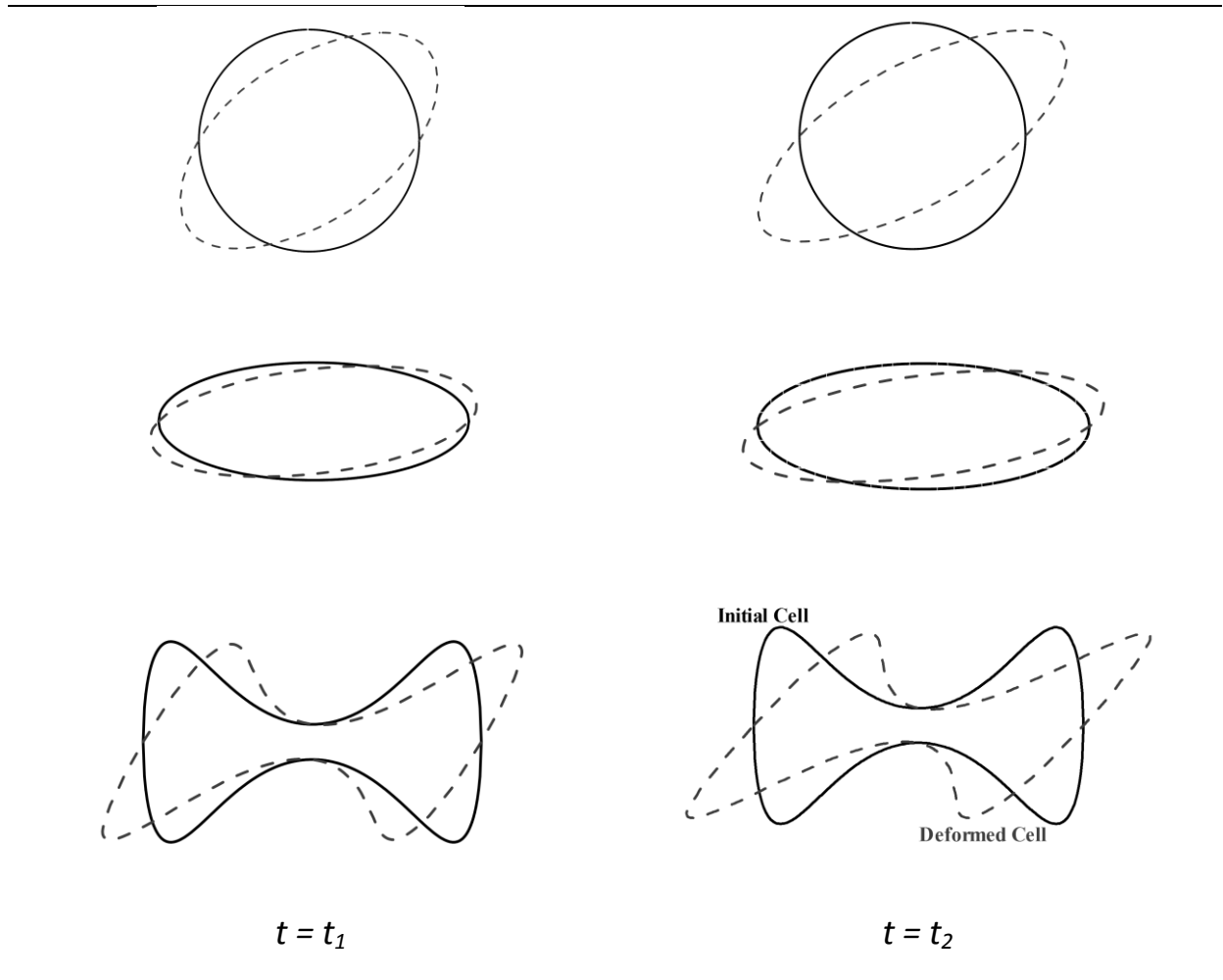


Figure 5: Deformation of the red blood cells with different geometry in shear flow

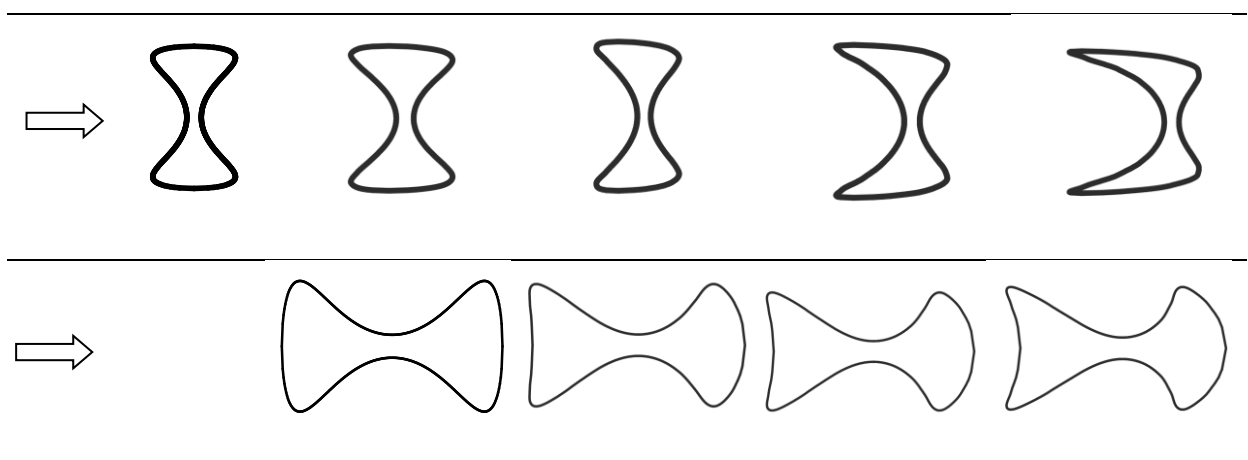


Figure 6: Deformation of red blood cells during the displacement in a channel

In figure 7 a carotid artery with complex geometry is selected for simulation the blood flow in a vessel. Streamlines in figure 7 (a) shown that good agreement between our simulation and the pervious results presented in [3, 6, 7, and 15]. The tissue will die because of the oxygen deficiency if the flow of blood in the blood vessel stopped. If after a serious injury blood flow on the outside of the body was not stopped, human will has died as a result of bleeding. However, usually the bleeding stops within a few minutes after cutting. Sometimes, the blood may clot, because of abnormal material floating in the blood vessel or damaged tissue. Any defect in the control of blood clotting factors can increase or decrease the risk of blood clots associated.. In this section the damaged tissue of artery is simulated in figure 7 (c). The obstruction of the artery and its effect on blood flow was shown by detail in this figure. As can be seen the obstruction in vessel causes to eddy formation and increases the chances of blood clots or the fat tissues accumulation in this area.

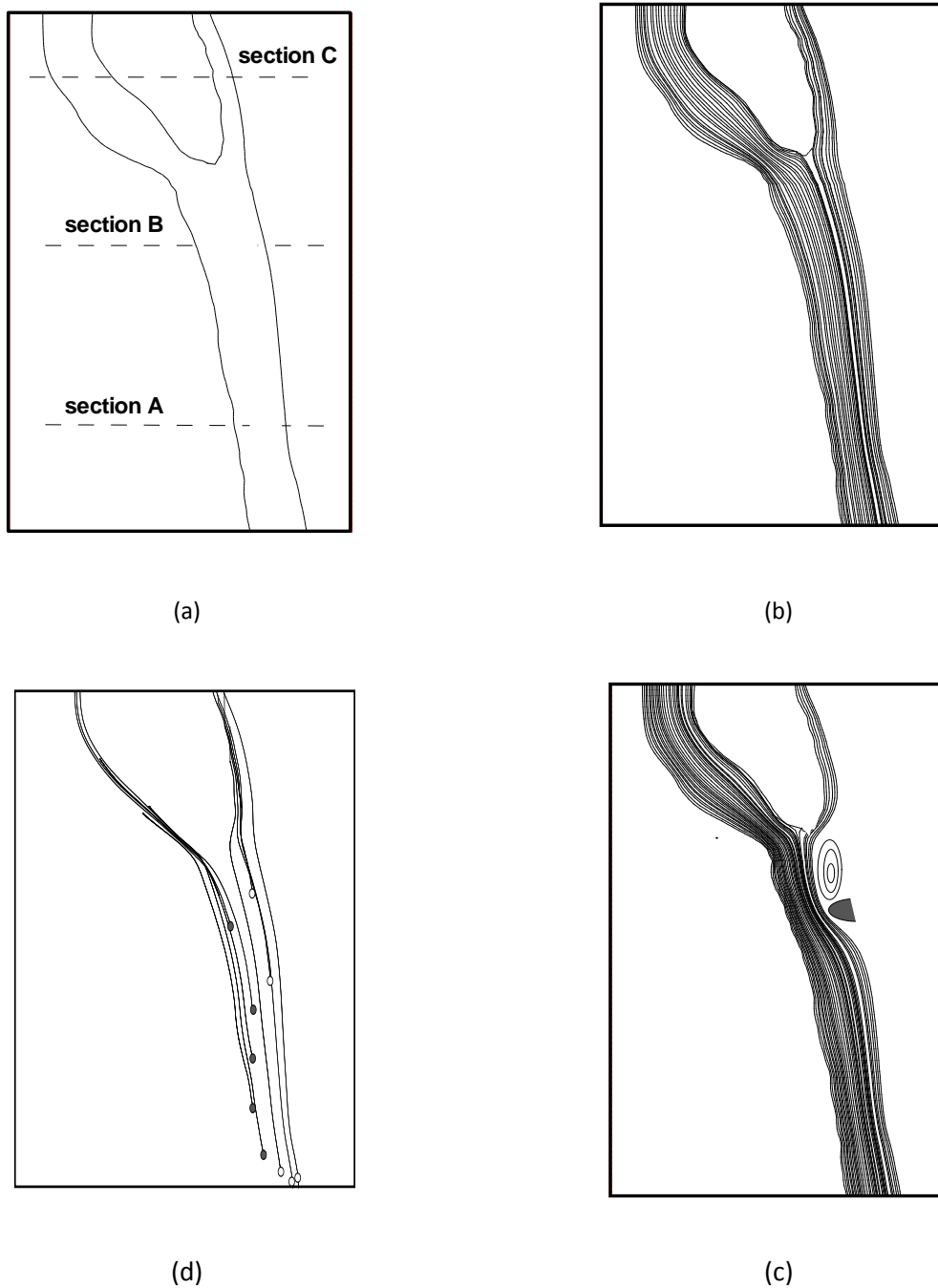


Figure 7: Streamline (a), different section of artery (b), obstruction(c), drug delivery (d)

Drug delivery includes medicinal compound transmission technology in a human body to achieve a desired therapeutic effect. In this process both quantities demanded and quality of medicinal materials are of great importance. Figure 7 (d) show the spherical particles have been released at different situation inside the artery. These situations were separated by different sections in figure 7 (b). As can be seen different released particles in different position have selected special paths for themselves. A closer examination of the results indicate that about 65% of the released particles before section A select the right branch and about 70% of the released particles between the section A and B chose the left branch to continue their motion path. These results indicate that by controlling the drug injection position in this artery the drug distribution quantity between two branches can be controlled.

CONCLUSION

The main goal of this study is to simulate the deformation of red blood cell and drug delivery in a blood vessel using lattice Boltzmann method (LBM). Compared with computational fluid dynamics methods, LBM can simulate difficult problems with complicated boundary conditions by a simple calculating procedure. In this research the flexibility of this method has been evaluated with different parameters. Some of the main achieved results are as follows:

- Composition of Immersed boundary method and LBM can properly simulate the deformation of red blood cells.
- Damage to the vessel wall can lead to the formation of vortices inside the arteries and block its path.
- Drug delivery path depends heavily on the quality of injection.

References

- [1] A. A. Mohammad, "Applied Lattice Boltzmann Method for Transport Phenomena Momentum Heat Mass Transfer," Univ. of Calgary Press, Calgary, 2007.
- [2] A. D'Orazio, M. Corcione, and G. P. Celata, "Application to natural convection enclosed flows of a lattice Boltzmann BGK model coupled with a general purpose thermal boundary condition," *International Journal of Thermal Sciences*, vol. 43, pp. 575–586, 2004.
- [3] A. S. Anayiotos, S. A. Jones, D. P. Giddens, S. Glagov, C. K. Zarins, "Shear stress at a compliant model of the human carotid bifurcation," *J. Biomech. Engng.*, vol. 117, pp. 98–106, 1994.
- [4] A. Mezrhab, Jami, M., Abid, C., Bouzidi, M., and Lallemand, P., "Lattice Boltzmann modeling of natural convection in an inclined square enclosure with partitions attached to its cold wall," *International Journal of Heat and Fluid Flow*, vol. 27, pp. 456–465, 2006.
- [5] B. Chopard, and P. O. Luthi, "Lattice Boltzmann computations and applications to physics," *Theoretical Computational Physics*, vol. 217, pp. 115–130, 1999.
- [6] B. K. Bharadvaj, R. F. Mabon, D. P. Giddens, "Steady flow in a model of the human carotid bifurcation—I. Flow visualization," *J. Biomech*, vol. 15, pp. 349–362, 1982.
- [7] B. K. Bharadvaj, R. F. Mabon, D. P. Giddens, "Steady flow in a model of the human carotid bifurcation—II. Laser-Doppler anemometer measurements," *J. Biomech*, vol. 15, pp. 363–378, 1982.
- [8] C. Shu, Y. Peng, and Y. T. Chew, "Simulation of natural convection in a square cavity by Taylor series expansion and least squares-based lattice Boltzmann method," *International Journal of Modern Physics*, vol. 13, pp. 1399–1414, 2002.
- [9] D. M. Aghajani, M. Farhadi, and K. Sedighi, "Effect of heater location on heat transfer and entropy generation in the cavity using the lattice Boltzmann method," *Heat Transfer Research*, vol. 40, pp. 521–536, 2009.
- [10] D. Yu, R. Mei, L. S. Luo, and W. Shyy, "Viscous flow computations with the method of lattice Boltzmann equation," *Progress in Aerospace Science*, vol. 39, No. 5, pp. 329–367, 2003.
- [11] J. A. Esfahani, J. Alinejad, "Lattice Boltzmann simulation of viscous-fluid flow and conjugate heat transfer in a rectangular cavity with a heated moving wall," *Thermo physics and Aeromechanics*, vol. 20, No. 5, pp. 613–620, 2013.
- [12] J. A. Esfahani, J. Alinejad, "Entropy generation of conjugate natural convection in enclosures: the Lattice Boltzmann Method," *Journal of Thermo physics and Heat Transfer*, vol. 27, No. 3, pp. 498–505, 2013.
- [13] N. Thürey and U. Rüdiger, "Stable free surface flows with the lattice Boltzmann method on adaptively coarsened grids," *Computing and Visualization in Science*, vol. 12, pp. 247–263, 2009.
- [14] P. Bagchi, P. C. Johnson, A. S. Popel, "Computational Fluid Dynamic Simulation of Aggregation of Deformable Cells in a Shear Flow," *J. Biomech. Engng.*, vol. 127, pp. 1070–1080, 2005.

- [15] R.H. Botnar, G. Rappitsch, M.B. Scheidegger, D. Liepsch, K. Perktold, P. Boesiger, "Hemodynamics in the carotid artery bifurcation: a comparison between numerical simulations and in vitro MRI measurements," *J.Biomech.* vol. 33, pp. 137–144, 2000.
- [16] R.Me, D.Yu,W. Shyy,L.Sh.Luo, "Force evaluation in the lattice Boltzmann method involving curved geometry," *Phys.Rev.* vol. E65, pp. 1-14, 2002.
- [17] R. R. Nourgaliev, T. N. Dinh, T. G. Theofanous, and D. Joseph, "The lattice Boltzmann equation method: theoretical interpretation, numerics and implications," *International Journal of Multiphase Flow*, vol. 29, No. 1, pp. 117–169, 2003.
- [18] S.A. Urquiza, P.J. Blanco, M.J. Vénere, and R.A. Feijóo, multidimensional modeling for the carotid blood flow, *Comput. Meth. Appl. Mech. Engrg.*, vol. 195, 2006, pp. 4002–4017.
- [19] T. Deschamps, P. Schwartz, D. Trebotichc, P. Colella, D. Saloner, R. Malladi, Vessel segmentation and blood flows emulation using Level-Sets and Embedded Boundary methods, *International Congress Series 1268 (2004)*75–80.
- [20] X. He, and L. S.Luo, "Lattice Boltzmann model for the incompressible Navier–Stokes equations," *Journal of Statistical Physics*, vol.88,Nos.3–4,pp.927–944,1997.
- [21] Z. Guo, and T. S. Zhao, "Lattice Boltzmann model for incompressible flows through porous media," *Physical Review*, vol. E66, pp. 036304, 2002.
- [22] Z.L.Guo,Ch.Zheng,B.C.Shi, "An extrapolation method for boundary conditions in lattice Boltzmann method," *Phys.Fluids*, vol. 14(6), pp. 2007-2010, 2002.